Negative axial radiation force on a fluid and elastic spheres illuminated by a high-order Bessel beam of progressive waves

2009 J. Phys. A: Math. Theor. 42 245202

(http://iopscience.iop.org/1751-8121/42/24/245202)

IOP PUBLISHING JOURNAL OF PHYSICS A: MATHEMATICAL AND THEORETICAL

J. Phys. A: Math. Theor. **42** (2009) 245202 (9pp) doi:10.1088/1751-8113/42/24/245202

Negative axial radiation force on a fluid and elastic spheres illuminated by a high-order Bessel beam of progressive waves

F G Mitri

Mayo Clinic College of Medicine, Department of Physiology and Biomedical Engineering, College of Medicine, 200 First Street SW, Rochester, MN 55905, USA

E-mail: mitri@ieee.org and mitri.farid@mayo.edu.

Received 9 February 2009
Published 26 May 2009
Online at stacks.iop.org/JPhysA/42/245202

Abstract

An analytical solution for the scattering of an acoustic Bessel beam of any order by a deformable sphere centered on the beam is used to calculate the acoustic radiation force acting along the wave propagation axis. Situations are noted where, even in the absence of absorption, the radiation force of a high-order Bessel beam acting on the sphere is *opposite* to the direction of beam propagation. In the present research, the cases of a *fluid* and solid *elastic* spheres are considered with particular emphasis on how the mechanical properties and resonances of spheres as well as the beam parameters affect the *negative* radiation force. Conditions for the negative attracting force on hexane (fluid), aluminum and gold spheres are established, which help in designing acoustic tweezers operating with high-order Bessel beams of progressive waves for potential applications in particle entrapment and manipulation.

PACS numbers: 43.20.−f, 43.25.−x, 43.25.Qp, 43.25.Uv, 43.80.Ev, 47.35.Rs.

(Some figures in this article are in colour only in the electronic version)

1. Introduction

Modern research using light Bessel beams has found breakthrough applications in the field of plasma physics [1], optics [2–5] for particle manipulation and entrapment [6, 7] and other fields, using the force of electromagnetic radiation [8–11]. Ideal Bessel beams are mathematical solutions of the Helmholtz equation that possess an azimuthal phase term of form $\exp(\pm im\phi)$, where m is the order of the beam and ϕ is the phase. Due to this property, such beams carry an orbital angular momentum that can be transferred to transparent particles of finite dimensions and set them into rotation [12]. Furthermore, Bessel beams do not

suffer from the diffractive nature of light. This property is a consequence of the way in which the beam depends on the spatial coordinates [13]. One additional property is their self-reconstruction ability [14]. Because the beam can be decomposed into a number of plane waves incident on an object placed in the center of the beam and traveling on the surface of a cone, the waves forming the beam propagate along the outside of the cone and hence are slightly affected by the diffraction of the object at the center. A high-order Bessel beam (HOBB) is therefore capable of retaining a tight focus on long sections of the beam. It is also able to resist against amplitude and phase distortions, and its transverse amplitude profile regenerates after the obstruction.

Similarly, in the field of acoustics, Bessel beams have therefore provided an attractive alternative to using Gaussian beams in a number of applications [15–22]. Recent theoretical research is currently investigating the feasibility of trapping spherical particles in the field of a Bessel beam [23–26]. However in all those prior studies, the beam was proportional to the *zero-order* Bessel function of the first kind J_0. Such a beam does not possess an azimuthal phase modulation ($m = 0$). Moreover, it has a bright central maximum intensity [3, 27], whereas a HOBB having a beam profile proportional to the Bessel functions J_m of the mth order possesses an axial phase singularity and hence has a non-diffracting dark central core (amplitude null). Due to this property, a HOBB is labeled as a 'hollow' or 'doughnut-shape' beam. The aim of this research is therefore directed toward extending the previous investigation on the radiation force experienced by a rigid sphere [26] to the case of elastic and fluid spheres immersed in non-viscous water and placed in a HOBB of *progressive* waves. The beam considered here has a phase ramp equal to $\exp(\pm \mathrm{i} m\phi)$. The total acoustic scattering field is solved first and then used to evaluate the radiation force. General properties and examples illustrating the theoretical analysis are discussed.

2. Acoustic radiation force of a HOBB on an elastic sphere

A HOBB of axisymmetric progressive waves is a solution of the linear Helmholtz equation for which the incident (complex) acoustic velocity potential may be expressed as [3, 27]

$$\Phi_{J_m,p}^{(\mathrm{inc})} = \Phi_0 \, \mathrm{e}^{\mathrm{i}(k_z z - \omega t)} J_m(k_r R) \, \mathrm{e}^{\pm \mathrm{i} m\phi}, \tag{1}$$

where Φ_0 is the amplitude, $k_z = k\cos\beta$ and $k_r = k\sin\beta$ are the axial and radial wave-numbers, respectively, $k = \sqrt{k_z^2 + k_r^2} = \omega/c = 2\pi/\lambda$ is defined as the wave number of the incident HOBB, ω is the angular frequency, c is the speed of sound in the fluid medium, λ is the wavelength of the acoustic radiation making up the HOBB, β is the half-cone angle formed by the wave-number k relative to the axis of wave propagation, and R, ϕ and z are the radial, azimuthal and axial components respectively. In the present theoretical analysis, the fluid is considered ideal (with no absorption) so that thermo-viscous effects and acoustic streaming are disregarded. However, analytical studies on the radiation forces of plane and spherical acoustic waves in thermo-viscous fluids [28–31] indicate that there are various situations where corrections to the radiation force may be significant especially in progressive waves. These studies generally support the conjecture that thermo-viscous corrections will be small when the oscillating viscous boundary layer thickness is much less than the sphere's radius. It is assumed that this condition holds for the situation considered here and the theory is still applicable in this limit.

In a system of spherical coordinates (r, θ, ϕ), the incident velocity potential may be expanded in a generalized Rayleigh wave series as [27, 32, 33]

$$\begin{aligned}\Phi^{(\mathrm{inc})}_{J_m,p} &= \Phi_0\,\mathrm{e}^{\mathrm{i}(k_z r\cos\theta-\omega t)}\,J_m(k_r r\sin\theta)\,\mathrm{e}^{\pm\mathrm{i}m\phi},\\ &= \Phi_0\,\mathrm{e}^{\mathrm{i}(kr\cos\beta\cos\theta-\omega t)}\,J_m(kr\sin\beta\sin\theta)\,\mathrm{e}^{\pm\mathrm{i}m\phi},\\ &= \Phi_0\,\mathrm{e}^{-\mathrm{i}\omega t}\sum_{n=m}^{\infty}\frac{(n-m)!}{(n+m)!}(2n+1)\mathrm{i}^{(n-m)}\,j_n(kr)\,P_n^m(\cos\theta)\,P_n^m(\cos\beta)\,\mathrm{e}^{\pm\mathrm{i}m\phi}. \qquad (2)\end{aligned}$$

The series in equation (2) is obtained by expanding the cylindrical Bessel function in a generalized partial wave series using the addition theorem for the associated Legendre functions (see page 412–413 and equation (82) in [32]—note the typeset error in the series that should start from $n = m$ to infinity). Equation (2) describes the velocity potential of a generalized HOBB incident upon a sphere, whose center is located at a distance r from an observation point, $j_n(\cdot)$ is the spherical Bessel function of order n, $P_n^m(\cdot)$ are the associated Legendre functions and θ is the scattering angle relative to the beam axis of wave propagation z.

When the incident wave, expressed by equation (2), acts on a sphere, the scattered spherical wave in the fluid surrounding the sphere may be expressed in terms of the spherical Hankel function of the first kind as follows [33]:

$$\Phi^{(sc)}_{J_m,p} = \Phi_0\,\mathrm{e}^{-\mathrm{i}\omega t}\sum_{n=m}^{\infty}\frac{(n-m)!}{(n+m)!}(2n+1)\mathrm{i}^{(n-m)}h_n^{(1)}(kr)A_n\,P_n^m(\cos\theta)\,P_n^m(\cos\beta)\,\mathrm{e}^{\pm\mathrm{i}m\phi}, \qquad (3)$$

where $h_n^{(1)}(\cdot)$ denotes the spherical Hankel function of the first kind, and the dimensionless (complex) scattering coefficients $A_n = (\alpha_n + \mathrm{i}\beta_n)$ for each partial wave are determined from the following boundary condition at the non-viscous water-elastic sphere interface: (i) the pressure (or velocity, respectively) in the fluid equals the normal component of stress in the solid at the interface, (ii) the normal (radial) component of displacement (or velocity, respectively) of the fluid must be equal to the normal component of displacement (or velocity, respectively) of the solid at the interface and (iii) the tangential components of shearing stress must vanish at the surface of the solid (since the exterior fluid medium is considered to be non-viscous). These functions depend on the sphere's material parameters such as the longitudinal sound speed $c_{\mathrm{L}} = \sqrt{(\lambda+2\mu)/\rho_{\mathrm{s}}}$, the shear or transverse sound speed $c_{\mathrm{T}} = \sqrt{\mu/\rho_{\mathrm{s}}}$, where λ and μ are the elastic and shear moduli, and the mass densities of both the fluid ρ and the sphere ρ_{s}. These coefficients are given in the appendix of [33] for elastic spheres.

From equations (2) and (3), the total (incident + scattered) velocity potential field is expressed by

$$\Phi^{(t)}_{J_m,p} = \Phi_0\,\mathrm{e}^{-\mathrm{i}\omega t}\sum_{n=m}^{\infty}\frac{(n-m)!}{(n+m)!}(2n+1)\mathrm{i}^{(n-m)}(U_n+\mathrm{i}V_n)\,P_n^m(\cos\theta)\,P_n^m(\cos\beta)\,\mathrm{e}^{\pm\mathrm{i}m\phi}, \qquad (4)$$

where U_n and V_n are given by the following equations:

$$U_n = (1+\alpha_n)\,j_n(kr) - \beta_n y_n(kr), \qquad V_n = \beta_n j_n(kr) + \alpha_n y_n(kr), \qquad (5)$$

where the function $y_n(\cdot)$ is the spherical Bessel function of the second kind, also known as the Neumann function.

The acoustic radiation force on the elastic sphere caused by a harmonic wave is defined as a *time-averaged* quantity over the period T, and is calculated by integrating the mean excess pressure over the surface of the sphere. Since the force is evaluated with accuracy up to second-order terms, it is therefore sufficient to integrate second-order quantities over the surface of the elastic sphere at rest. With accuracy up to second-order terms in the excess of pressure, the averaged force on the elastic sphere may be expressed as [34]

$$\langle\mathbf{F}\rangle = \left\langle\iint_s \mathscr{L}\,\mathbf{n}\,\mathrm{d}S\right\rangle_T - \left\langle\iint_s \rho\mathbf{v}^{(1)}v_n\,\mathrm{d}S\right\rangle, \qquad (6)$$

where

$$\begin{aligned}\mathscr{L} &= (\rho/2)\left|\nabla\left(\Psi^{(t)}_{J_m,p}\right)^{(1)}\right|^2 - (\rho/2c^2)\left[\partial_t\left(\Psi^{(t)}_{J_m,p}\right)^{(1)}\right]^2 \\ &= \mathscr{K} - \mathscr{U} \end{aligned} \tag{7}$$

is the Lagrangean energy density, $\partial_t = \partial/\partial t$, $\Psi^{(t)}_{J_m,p} = \mathrm{Re}\left[\Phi^{(t)}_{J_m,p}\right]$, the superscript (1) denotes first-order quantities and $\mathbf{n}$ is the outward-pointing unit normal vector of $\mathrm{d}S = r^2 \sin\theta\, \mathrm{d}\theta\, \mathrm{d}\phi$. Denoting the first-order fluid particle velocity $\mathbf{v}^{(1)} = v_n\mathbf{n} + v_t\mathbf{t}$, where $\mathbf{t}$ is the unit tangential vector of $\mathrm{d}S$, the two components of $\mathbf{v}^{(1)}$ are given in terms of $\left(\Psi^{(t)}_{J_m,p}\right)^{(1)}$ as $v_n = -\partial_r\left(\Psi^{(t)}_{J_m,p}\right)^{(1)}$ and $v_t = -\partial_\theta\left(\Psi^{(t)}_{J_m,p}\right)^{(1)}/r$ respectively. Then the components of $\mathbf{n}$ and $\mathbf{t}$ in the direction of the incident waves are $\cos\theta$ and $-\sin\theta$ respectively.

In the direction of wave propagation (axial z-direction), the radiation force on the sphere can therefore be expressed as

$$\langle F_z\rangle_{J_m,p} = \langle F_r\rangle_{J_m,p} + \langle F_\theta\rangle_{J_m,p} + \langle F_\phi\rangle_{J_m,p} + \langle F_{r,\theta}\rangle_{J_m,p} + \langle F_t\rangle_{J_m,p}, \tag{8}$$

where

$$\begin{aligned}
\langle F_r\rangle_{J_m,p} &= (-a^2\rho/2)\left\langle \int_0^{2\pi}\left\{\int_0^{\pi}\left[\partial_r\left(\Psi^{(t)}_{J_m,p}\right)^{(1)}\right]^2_{r=a}\sin\theta\cos\theta\,\mathrm{d}\theta\right\}\mathrm{d}\phi\right\rangle, \\
\langle F_\theta\rangle_{J_m,p} &= (\rho/2)\left\langle \int_0^{2\pi}\left\{\int_0^{\pi}\left[\partial_\theta\left(\Psi^{(t)}_{J_m,p}\right)^{(1)}\right]^2_{r=a}\sin\theta\cos\theta\,\mathrm{d}\theta\right\}\mathrm{d}\phi\right\rangle, \\
\langle F_\phi\rangle_{J_m,p} &= (\rho/2)\left\langle \int_0^{2\pi}\left\{\int_0^{\pi}\left[\partial_\phi\left(\Psi^{(t)}_{J_m,p}\right)^{(1)}\right]^2_{r=a}\cot\theta\,\mathrm{d}\theta\right\}\mathrm{d}\phi\right\rangle, \\
\langle F_{r,\theta}\rangle_{J_m,p} &= (a\rho)\left\langle \int_0^{2\pi}\left\{\int_0^{\pi}\left[\partial_r\left(\Psi^{(t)}_{J_m,p}\right)^{(1)}\right]_{r=a}\left[\partial_\theta\left(\Psi^{(t)}_{J_m,p}\right)^{(1)}\right]_{r=a}\sin^2\theta\,\mathrm{d}\theta\right\}\mathrm{d}\phi\right\rangle, \\
\langle F_t\rangle_{J_m,p} &= (-a^2\rho/2c^2)\left\langle \int_0^{2\pi}\left\{\int_0^{\pi}\left[\partial_t\left(\Psi^{(t)}_{J_m,p}\right)^{(1)}\right]^2_{r=a}\sin\theta\cos\theta\,\mathrm{d}\theta\right\}\mathrm{d}\phi\right\rangle.
\end{aligned} \tag{9}$$

The total velocity potential field given in equation (4) may be rewritten as

$$\Psi^{(t)}_{J_m,p} = \mathrm{Re}\left[\Phi^{(t)}_{J_m,p}\right] = \Phi_0\sum_{n=m}^{\infty}(2n+1)R^m_n P^m_n(\cos\theta), \tag{10}$$

where $R^m_n = \mathrm{Re}\left[\mathrm{i}^n(U_n(kr) + \mathrm{i}V_n(kr))\Lambda^m_{n,p}\,\mathrm{e}^{-\mathrm{i}\omega t}\right]$ and $\Lambda^m_{n,p} = \mathrm{i}^{-m}\frac{(n-m)!}{(n+m)!}P^m_n(\cos\beta)\,\mathrm{e}^{\pm\mathrm{i}m\phi}$.

Substituting equation (10) into equation (9), manipulating the results using the properties of the associated Legendre functions (equations (68) and (72) in [35]) and the time average of a product [36], and denoting by $E = \rho k^2|\Phi_0|^2/2$ the characteristic energy density, the final expression for the *axial* radiation force given by equation (8) is simplified and expressed by

$$\langle F_z\rangle_{J_m,p} = Y_{J_m,p}\,S_c E, \tag{11}$$

where $S_c = \pi a^2$ is the cross-sectional area. The dimensionless factor $Y_{J_m,p}$ is defined as the radiation force function for a HOBB of progressive waves, which is the radiation force per unit energy density and unit cross-sectional surface. Its expression is given by

$$Y_{J_m,p} = -\frac{4}{(ka)^2}\sum_{n=m}^{\infty}\left\{\begin{array}{l}\dfrac{(n-m+1)!}{(n+m)!}[\alpha_n + \alpha_{n+1} + 2(\alpha_n\alpha_{n+1} + \beta_n\beta_{n+1})] \\ \times P^m_n(\cos\beta)\,P^m_{n+1}(\cos\beta)\end{array}\right\}, \tag{12}$$

where coefficients α_n and β_n are the real and imaginary parts of the scattering coefficients A_n given in the appendix of [33].

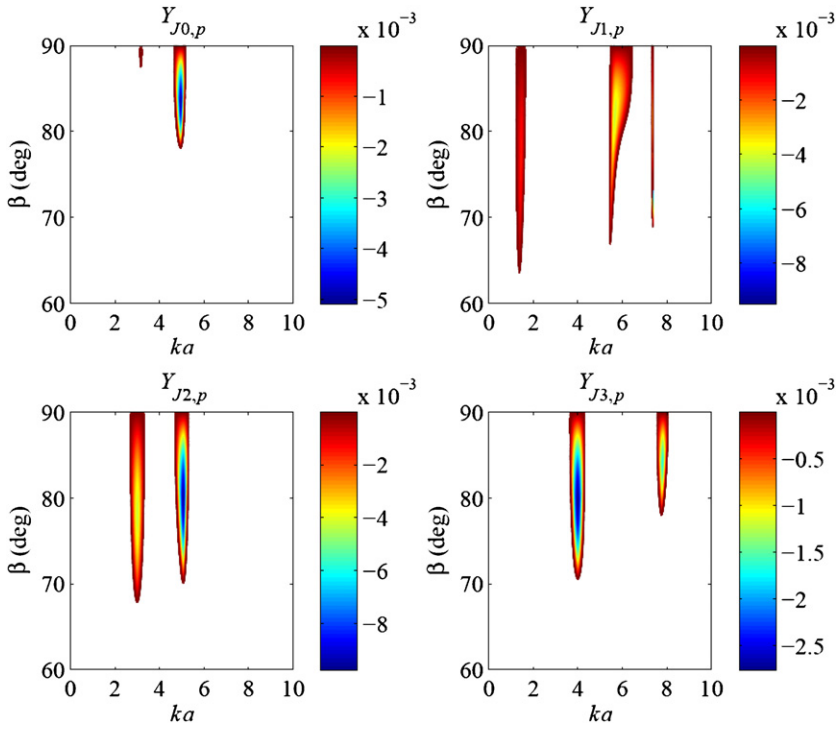

Figure 1. The 2D plots where $Y_{J_m,p}$ are computed by equation (12) to be negative are shown as 'islands' bounded by a contour at $Y_{J_m,p} = 0$. The plots are computed for zero-($Y_{J_0,p}$), first-($Y_{J_1,p}$), second-($Y_{J_2,p}$) and third-($Y_{J_3,p}$) order Bessel beams for an aluminum sphere immersed in water. One particularly notices the appearance of enlarged 'island' areas over which $Y_{J_m,p}$ is negative for HOBBs ($m > 0$). Note that the amplitude scale bar changes when the order of the HOBB increases from $m = 0$ to $m = 3$.

3. Numerical results and discussion

Example calculations for the radiation force function as given by equation (12) are initially evaluated for elastic aluminum ($\rho_{s,Al} = 2700$ kg m^{-3}, $c_{L,Al} = 6420$ m s^{-1}, $c_{T,Al} = 3040$ m s^{-1}) and gold ($\rho_{s,Au} = 19\,300$ kg m^{-3}, $c_{L,Au} = 3240$ m s^{-1}, $c_{T,Au} = 1200$ m s^{-1}) spheres immersed in water ($\rho = 1000$ kg m^{-3}, $c = 1500$ m s^{-1}). A MATLAB [37] code is constructed to calculate the scattering coefficients as well as the acoustic radiation force function versus the non-dimensional frequency ka, the half-cone angle β and the order m of the HOBB. The computations are performed on a Pentium 4 personal computer with the maximum index N (=30) in the series in equation (12) to largely exceed ka to ensure proper convergence in the higher ka range. The 2D plots of the radiation force function $Y_{J_m,p}$ are computed in the range $\begin{cases} 0 \leqslant ka \leqslant 10 \\ 60^\circ \leqslant \beta \leqslant 90^\circ \end{cases}$. The computational increment of $\Delta ka = 10^{-3}$ is used for an adequate detection of the resonance peaks. As an initial test, calculations for $Y_{J_m,p}$ are performed for the case of a plane wave ($m = 0$, $\beta = 0$) and a zero-order Bessel progressive wave ($m = 0$), which show excellent agreement with previous investigations involving plane wave illumination [38] and zero-order Bessel beams [23].

The $Y_{J_m,p}$ plots for an aluminum sphere in water are shown in figure 1 for a Bessel beam of zero-($Y_{J_0,p}$), first-($Y_{J_1,p}$), second-($Y_{J_2,p}$) and third-($Y_{J_3,p}$) orders, respectively. Only the

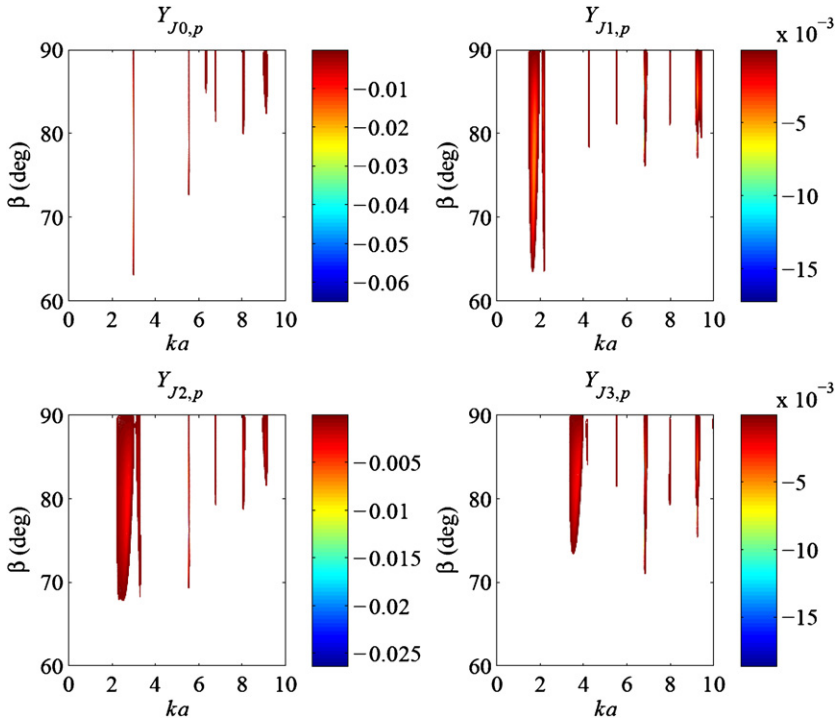

Figure 2. The same as in figure 1, but for a gold sphere immersed in water. One particularly notices the appearance of sharp 'islands' (versus ka) over which the $Y_{J_m,p}$ plots are negative. Gold spheres immersed in water are known to exhibit successive sharp resonances when subjected to incident acoustic plane waves. In the cases shown here, resonances are extremely sensitive to the mechanical properties of the object under test as well as the HOBB parameters. Note that the amplitude scale bar changes when the order of the HOBB increases from $m = 0$ to $m = 3$.

'islands' over which the radiation force function is negative for specific values of ka and β are shown. For $m = 1$, one particularly notices the sharp 'island' (for $ka \approx 7.3$) over which the $Y_{J_1,p}$ plot is negative. In addition, the sharp island is suppressed and a decrease in the areas of the remaining islands is also noticed as the order of the Bessel beam increases (from $m = 1$ to 3).

Figure 2 shows the $Y_{J_m,p}$ plots for a gold elastic sphere immersed in water. One particularly notices the sharp 'islands' (versus ka) over which $Y_{J_m,p}$ plots are negative. This typical example shows additional features; gold spheres immersed in water are known to exhibit successive sharp resonances when subjected to incident plane acoustic waves [39]. Resonances are extremely sensitive to the mechanical properties of the object under test, and they can be manifested as maxima and minima peaks [40]. To provide a theoretical explanation of this phenomenon, it is essential to introduce the concept of the scattering cross-section that characterizes the scattering strength of the elastic sphere, thus the radiation force. When the incident HOBB strikes the elastic sphere, it generates a surface wave that is propagated on its surface [41]. This wave decays progressively and reradiates a bulk wave in the fluid medium surrounding the sphere. The bulk wave interferes with the outer surface wave resulting in maxima and minima peaks in the resonance spectrum. Hence, when bulk waves are out of phase with the outer surface wave, resonance appears as minima instead of maxima peaks in the total scattering cross section curves. Moreover, the width of any resonance peak is related to the time which surface waves spend inside the sphere to be transformed to bulk waves. This

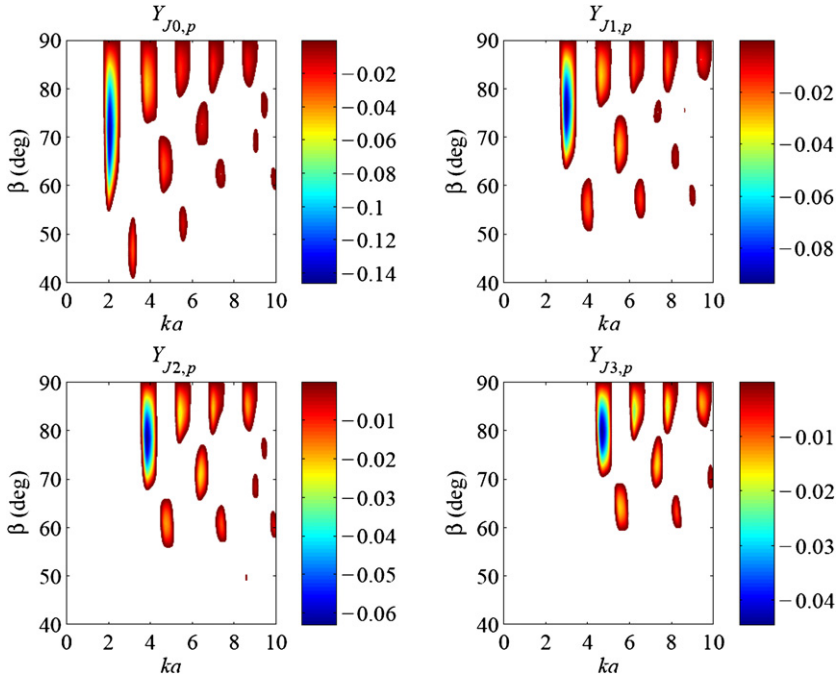

Figure 3. The same as in figure 1, but for an ideal fluid hexane sphere immersed in water. The multiple number of islands over which the $Y_{J_m,p}$ plots are negative versus figures 1 and 2 is particularly noticeable. As the order of the Bessel beam increases, the negative radiation force function amplitude decreases. In addition, as ka and β increase, the areas over which the $Y_{J_m,p}$ plots are negative decrease as well. Note that the amplitude scale bar changes when the order of the HOBB increases from $m = 0$ to $m = 3$.

period is known as the 'dwell time' [42] in optical resonance scattering. So, for sharp peaks, surface waves are rapidly attenuated to create bulk waves.

Figure 3 shows the $Y_{J_m,p}$ plots for an ideal fluid hexane ($\rho_{s,C_6H_{14}} = 656$ kg m^{-3}, $c_{L,C_6H_{14}} = 1078.5$ m s^{-1}) sphere immersed in water in the range $\begin{cases} 0 \leqslant ka \leqslant 10 \\ 40^\circ \leqslant \beta \leqslant 90^\circ \end{cases}$. In an ideal fluid sphere, shear wave propagation is absent, and therefore $c_{T,C_6H_{14}} = 0$. The plot $Y_{J_0,p}$ shows excellent agreement with a prior study dealing with the interaction of a *zero-order* Bessel beam with a hexane sphere in water [23]. The multiple number of islands over which the $Y_{J_m,p}$ plots are negative is also noticeable. As the order of the Bessel beam increases, the negative radiation force function amplitude decreases. In addition, as ka and β increase, the areas over which the $Y_{J_m,p}$ plots are negative decrease as well.

Further mathematical analysis of equation (12) shows the direct dependence on the associated Legendre functions $P_n^m(\cos\beta)$. It is therefore convenient to define $\beta^{(n,m)}$ as the root(s) of the associated Legendre functions $P_n^m(\cos\beta^{(n,m)}) = 0$, which are listed in table 1, for $0^\circ < \beta^{(n,m>0)} < 90^\circ$, and $n = 3, \ldots, 10$. The specific angles $\beta^{(n,m)}$ are associated with the nth partial waves. Suppressing the contribution of a particular resonance to the radiation force function is therefore attainable by appropriate selection of the half-cone angle β to correspond to $\beta^{(n,m)}$. This has been confirmed in suppressing the hexapole resonance ($n = 3$, $m = 0$) of a polyethylene elastic sphere [25] placed in *zero-order* Bessel beam tweezers. The extension for the case of a HOBB by judiciously selecting the half-cone angle to correspond to a root of $P_n^m(\cos\beta^{(n,m)}) = 0$ is therefore feasible.

Table 1. Roots of the associated Legendre functions $P_n^m(\cos\beta^{(n,m)}) = 0$. Only the roots $0^\circ < \beta^{(n,m)0)} < 90^\circ$ are listed.

n	m $\neq 0$	β (°)	n	m $\neq 0$	β (°)
3	1	63.4349			42.3729
4	1	49.1066			61.45
4	2	67.7923			80.4865
5	1	40.0880	9	2	31.1958
		73.4273			51.143
5	2	54.7356			70.6322
5	3	70.5287	9	3	39.1463
6	1	33.8782			59.9395
		62.0404			80.0285
6	2	45.9929	9	4	47.2657
		75.4891			69.0589
6	3	58.5178	9	5	55.8163
6	4	72.4515			78.8691
7	1	29.3385	9	6	65.1601
		53.7222	9	7	75.9637
		77.9187	10	1	20.9325
7	2	39.6949			38.3270
		65.1076			55.5813
7	3	50.1602			72.7969
		76.9331	10	2	28.1872
7	4	61.2894			46.2065
7	5	73.8978			63.8046
8	1	25.8737			81.2785
		47.3758	10	3	35.3022
		68.7082			54.0374
8	2	34.9306			72.1116
		57.2751	10	4	42.4925
		79.1243			62.0370
8	3	43.9550			80.7391
		67.3394	10	5	49.9406
8	4	53.3157			70.4369
		78.0169	10	6	57.863
8	5	63.4349			79.5619
8	6	75.0367	10	7	66.5867
9	1	23.1419	10	8	76.7373

4. Summary

An analytical expression for the radiation force function of a HOBB of progressive waves incident upon submerged elastic and fluid spheres placed along the waves' axis is derived. The analysis is based on solving the problem of acoustic scattering that is used to evaluate the force of a HOBB having an azimuthal dependence on phase. With appropriate selection of the dimensionless frequency *ka*, the half-cone angle β and the order *m* of the HOBB, the force exerted on the sphere is a force of attraction. The ability to trap or pull back toward the

source of a *single* HOBB may be therefore attainable. In addition, specific half-cone angles $\beta^{(n,m)}$ judiciously chosen may be used for suppressing selective resonances corresponding to the contribution of *n*th partial waves. These conditions are important in designing acoustical tweezers operating with HOBBs of progressive waves in various fields of applications.

References

[1] Fan J, Parra E, Alexeev I, Kim K Y, Milchberg H M, Margolin L Y and Pyatnitskii L N 2000 *Phys. Rev.* E **62** R7603
[2] Bouchal Z 2003 *Czech. J. Phys.* **53** 537
[3] Mcgloin D and Dholakia K 2005 *Contemp. Phys.* **46** 15
[4] Dholakia K and Lee W M 2008 *Adv. At. Mol. Opt. Phys.* **56** 261
[5] Grier D G 2003 *Nature* **424** 810
[6] Garces-Chavez V, Mcgloin D, Melville H, Sibbett W and Dholakia K 2002 *Nature* **419** 145
[7] Garces-Chavez V, Roskey D, Summers M D, Melville H, Mcgloin D, Wright E M and Dholakia K 2004 *Appl. Phys. Lett.* **85** 4001
[8] Ashkin A 1970 *Phys. Rev. Lett.* **24** 156
[9] Klima R and Petrzilka V A 1975 *J. Phys. A: Math. Gen.* **8** 829
[10] Klima R and Petrzilka V A 1978 *J. Phys. A: Math. Gen.* **11** 1687
[11] Ashkin A 1997 *Proc. Natl Acad. Sci.* **94** 4853
[12] Volke-Sepulveda K, Garces-Chavez V, Chavez-Cerda S, Arlt J and Dholakia K 2002 *J. Opt.* B **4** S82
[13] Lopez-Mariscal C and Gutierrez-Vega J C 2007 *Am. J. Phys.* **75** 36
[14] Bouchal Z, Wagner J and Chlup M 1998 *Opt. Commun.* **151** 207
[15] Hsu D K, Margetan F J and Thompson D O 1989 *Appl. Phys. Lett.* **55** 2066
[16] Campbell J A and Soloway S 1990 *J. Acoust. Soc. Am.* **88** 2467
[17] Lu J Y, Song T K, Kinnick R R and Greenleaf J F 1993 *IEEE Trans. Med. Imaging* **12** 819
[18] Nagai K, Monma H and Mizutani K 1993 *Japan. J. Appl. Phys.* **1 32** 2295
[19] Lu J Y 1997 *IEEE Trans. Ultrason. Ferroelectr. Freq. Control* **44** 181
[20] Masuyama H, Yokoyama T, Nagai K and Mizutani K 1999 *Japan. J. Appl. Phys.* **1 38** 3080
[21] Stepanishen P R 1999 *J. Acoust. Soc. Am.* **105** 1493
[22] Fox P D and Holm S 2002 *IEEE Trans. Ultrason. Ferroelectr. Freq. Control* **49** 85
[23] Marston P L 2006 *J. Acoust. Soc. Am.* **120** 3518
[24] Mitri F G 2008 *Ann. Phys.* **323** 1604
[25] Mitri F G and Fellah Z E A 2008 *IEEE Trans. Ultrason. Ferroelectr. Freq. Control* **55** 2469
[26] Mitri F G 2009 *IEEE Trans. Ultrason. Ferroelectr. Freq. Control* **56** 1059
[27] Mitri F G 2008 *Ann. Phys.* **323** 2840
[28] Doinikov A A 1997 *J. Acoust. Soc. Am.* **101** 713
[29] Doinikov A A 1997 *J. Acoust. Soc. Am.* **101** 722
[30] Doinikov A A 1997 *J. Acoust. Soc. Am.* **101** 731
[31] Danilov S D and Mironov M A 2000 *J. Acoust. Soc. Am.* **107** 143
[32] Stratton J A 1941 *Electromagnetic Theory* (New York: McGraw-Hill)
[33] Mitri F G 2009 *IEEE Trans. Ultrason. Ferroelectr. Freq. Control* **56** 1100
[34] Yosioka K and Kawasima Y 1955 *Acoustica* **5** 167
[35] http://Mathworld.Wolfram.Com/Legendrepolynomial.Html
[36] Temkin S 2001 *Elements of Acoustics* (Melville, NY: Acoustical Society of America)
[37] Matlab http://www.mathworks.com/
[38] Hasegawa T and Yosioka K 1969 *J. Acoust. Soc. Am.* **46** 1139
[39] Chivers R C and Anson L W 1982 *Ultrasonics* **20** 25
[40] Mitri F G and Chen S G 2005 *Phys. Rev.* E **71** 016306
[41] Uberall H 1973 *Phys. Acoust.* **10** 1
[42] Lagendijk A and Van Tiggelen B A 1996 *Phys. Rep.* **270** 143